A New Lindqvist Polyanion-based Three-dimensional Network with a NaCl Topology

Shaobin Li[a,b], Haijun Pang[a], Huiyuan Ma[a,b], Kun Wang[a], and Chuncheng Zhu[b]

[a] Key Laboratory of Green Chemical Engineering and Technology of College of Heilongjiang Province, College of Chemical and Environmental Engineering, Harbin University of Science and Technology, Harbin 150040, P. R. China
[b] Chemistry Department, Harbin Normal University, Harbin 150025, P. R. China

Reprint requests to Huiyuan Ma. Tel.: 86-0451-86392716. Fax: 86-0451-86392716.
E-mail: mahy017@163.com, or
Chuncheng Zhu. Tel.: 86-0451-88060623. Fax: 86-0451-88060085.
E-mail: zhuccshs@yahoo.com.cn

A new compound $[Co(bipy)_3][Mo_6O_{19}] \cdot H_2O$ (**1**) (bipy = 2,2′-bipyridine) has been synthesized under hydrothermal conditions and characterized by IR spectroscopy, TG analysis and single-crystal X-ray diffraction. The crystal structure consists of a $[Co(bipy)_3]^{2+}$ cation, an $[Mo_6O_{19}]^{2-}$ anion, and a water molecule. In **1** each $[Co(bipy)_3]^{2+}$ cation is surrounded by six $[Mo_6O_{19}]^{2-}$ anions and *vice versa* in a cubic face-centered close packing array, forming a 3D architecture with NaCl topology. Cations and anions are connected *via* weak hydrogen bonds in which also the water molecule participates. The luminescent and electrochemical properties of the title compound have also been studied.

Key words: Polyoxometalates, NaCl Topology, Lindqvist-type Structure, Electrochemical and Luminescent Properties

Introduction

Polyoxometalates (POMs) [1 – 3] are an outstanding class of nanosized metal oxoanions with wide structural diversity and interesting properties that have potential applications in catalysis [4 – 6], medicine [7, 8] and materials science [9, 10]. Recently, a widespread interest in POM chemistry has focused on the modification and functionalization of polyoxoanions by transition metal complexes (TMCs) through the design and synthesis of novel hybrid compounds that bear features of both inorganic and organic components and extend the structural multiplicity and versatility of POMs. A variety of such organic-inorganic hybrid materials have been successfully prepared by using proper POMs and TMCs as building blocks [11, 12].

In the various POMs, polyoxomolybdates are a remarkable family for their diverse structures, from the small di-, tri-, tetra-, and hexamolybdate to the medium-nuclearity octamolybdate and the $[H_2Mo_{16}O_{52}]^{10-}$ unit, finally up to the ultra-large 'lemon' shaped $\{Mo_{368}\}$ cluster [13]. As a ramification, the hexamolybdate anion $[Mo_6O_{19}]^{2-}$ (Lindqvist-type structure) is a classic POM. So far, many compounds based on Lindqvist-type polyoxomolybdates have been reported [14 – 23]. However, among these examples, the compounds constructed with TMCs are few [14, 15, 18, 19, 21]. Therefore, it is still worthwhile to design and synthesize novel architectures.

In this work, we chose the $[Mo_6O_{19}]^{2-}$ dianion and cobalt(II)/bipyridyl cations to construct new compounds by using the *insitu* synthetic strategy, and were successful in isolating a new inorganic-organic hybrid compound, $[Co(bipy)_3][Mo_6O_{19}] \cdot H_2O$ (**1**). Compound **1** represents a new 3D network with an interesting NaCl topology. Also, it exhibits not only good electrocatalytic activities for the reduction of H_2O_2 and IO_3^-, but also luminescent properties.

Experimental Section

Materials and methods

All chemicals were of reagent grade and used without further purification. Elemental analyses (C, H and N) were performed on a Perkin-Elmer 2400 CHN Elemental Analyzer. The FT-IR spectra were recorded from KBr pellets in the range $4000 – 400$ cm^{-1} with a Nicolet AVATAR FT-IR360 spectrometer. TG analysis was performed on a Perkin Elmer

Table 1. Crystal data and structure refinement for **1**.

Empirical formula	$C_{30}H_{26}CoMo_6N_6O_{20}$
M_r	1425
Color, habit	yellow, block
Crystal size, mm^3	$0.46 \times 0.44 \times 0.34$
Crystal system; space group	cubic; $P2_13$
$a = b = c$, Å	15.7518(3)
V, Å^3	3908.32(13)
Z	4
D_{calcd}, g cm^{-3}	2.42
$\mu(\text{Mo}K_\alpha)$, cm^{-1}	28.3
$F(000)$, e	2740.0
hkl range	$-21 \leq h \leq 20$, $-20 \leq k \leq 17$, $-20 \leq l \leq 21$
Absorption correction	empirical
Refl. measured / unique / R_{int}	29426 / 3258 / 0.0255
Data / ref. parameters	3255 / 190
R_1 / wR_2 $[I \geq 2\sigma(I)]^{a,b}$	0.0335 / 0.0938
R_1 / wR_2 (all data)	0.0380 / 0.1000
Flack parameter	0.02(4)
GoF $(F^2)^c$	0.973
$\Delta\rho_{fin}$ (max / min), e Å^{-3}	1.06 / -0.74

^{a} $R_1 = \Sigma||F_o| - |F_c||/\Sigma|F_o|$; ^{b} $wR_2 = [\Sigma w(F_o^2 - F_c^2)^2/\Sigma w(F_o^2)^2]^{1/2}$, $w = [\sigma^2(F_o^2) + (AP)^2 + BP]^{-1}$, where $P = (\text{Max}(F_o^2, 0) + 2F_c^2)/3$; ^{c} GoF $= [\Sigma w(F_o^2 - F_c^2)^2/(n_{obs} - n_{param})]^{1/2}$.

Diamond TG-DTA 6300 thermal analyzer in air with a heating rate of 10 °C min^{-1}. A CHI660 electrochemical workstation was used for control of the electrochemical measurements and data collection. A conventional three-electrode system was used, with a carbon paste electrode (CPE) as a working electrode, a commercial Ag/AgCl as reference electrode and a twisted platinum wire as counter electrode.

*Synthesis of $[Co(bipy)_3][Mo_6O_{19}] \cdot H_2O$ (**1**)*

Compound **1** was prepared under hydrothermal conditions in 62 % yield (based on Mo). A mixture of 0.2 g Na$_2$Mo$_4$·H$_2$O, 0.1 g CoCl$_2$·6H$_2$O, 0.04 g NH$_4$VO$_3$, 0.05 g bipy and 15 mL H$_2$O (molar ratio of 2 : 1 : 1 : 1 : 2000) was stirred for 30 min at 50 °C. Then the solution was sealed in a 23 mL Teflon-lined autoclave and heated at 165 °C for 5 d with a starting pH = 4.3 adjusted by 6 M HCl. After cooling slowly to room temperature, dark-yellow block-shaped crystals were obtained. The crystals were filtered and dried at room temperature. Elemental analysis (%): calcd. C 25.28, H 1.83, O 22.45, N 5.89, Co 4.13, Mo 40.39; found C 25.13, H 1.78, O 22.56, N 5.93, Co 4.09, Mo 40.31.

X-Ray crystallography

A single crystal of **1** was carefully selected for single-crystal X-ray diffraction analysis. Data collection was performed on a Rigaku RAXIS-RAPID equipped with a narrow-focus, 5.4 kW sealed tube with graphite-monochromated MoK_α radiation ($\lambda = 0.71073$ Å). The data were collected at

Table 2. Selected bong lengths (Å) for compound **1**.

Mo(1)–O(3)	2.319(3)	Mo(1)–O(4)	1.880(4)
Mo(1)–O(5)	1.877(5)	Mo(1)–O(6)	1.694(4)
Mo(2)–O(1)	1.674(4)	Mo(2)–O(2)	1.856(3)
Mo(2)–O(3)	2.278(3)	Mo(2)–O(4)	1.983(3)
Mo(2)–O(7)	1.863(4)		
Co(2)–N(1)	1.944(4)	Co(2)–N(2)	1.923(4)

Table 3. Selected bond angles (deg) for compound **1**.

O(6)–Mo(1)–O(5)	105.2(2)	O(4)–Mo(1)–O(5)	91.2(2)
O(6)–Mo(1)–O(4)	104.0(2)	O(6)–Mo(1)–O(3)	176.72(19)
O(4)–Mo(1)–O(3)	77.53(13)	O(5)–Mo(1)–O(3)	77.63(16)
O(1)–Mo(2)–O(2)	103.96(17)	O(1)–Mo(2)–O(7)	101.85(19)
O(2)–Mo(2)–O(7)	92.08(17)	O(1)–Mo(2)–O(4)	100.20(17)
O(2)–Mo(2)–O(4)	155.63(14)	O(7)–Mo(2)–O(4)	86.02(17)
O(1)–Mo(2)–O(3)	176.80(16)	O(2)–Mo(2)–O(3)	79.22(13)
O(7)–Mo(2)–O(3)	78.12(15)	O(4)–Mo(2)–O(3)	76.60(13)

a temperature of 20 ± 2 °C. The data processing was accomplished with the program PROCESS-AUTO. The structure was solved by Direct Methods and refined by full-matrix least-squares on F^2 using the SHELXTL-97 crystallographic software package. Anisotropic displacement parameters were used to refine all non-hydrogen atoms. The organic hydrogen atoms were generated geometrically. The hydrogen atoms of the water molecule in **1** could not be refined but were included in the structure factor calculation. Further details of the X-ray structure analysis are given in Table 1. Selected bond lengths and angles are listed in Tables 2 and 3, respectively.

CCDC 783483 contains the supplementary crystallographic data for this paper. These data can be obtained free of charge from The Cambridge Crystallographic Data Centre *via* www.ccdc.cam.ac.uk/data_request/cif.

Results and Discussion

Description of the structure

The single-crystal X-ray diffraction analysis has shown that **1** consists of one Lindqvist anion $[Mo_6O_{19}]^{2-}$, one $[Co(bipy)_3]^{2+}$ cation and one water molecule (Fig. 1). The structure of the $[Mo_6O_{19}]^{2-}$ anion displays the well-known characteristics consisting of six MoO$_6$ octahedra with three distinct types of Mo–O bond lengths, *viz.* terminal oxygen atoms, O$_t$ bridging oxygen atoms, O$_b$ and central oxygen atoms O$_c$. The average distances of 2.318, 1.924 and 1.685 Å for Mo–O$_t$ Mo–O$_b$ and Mo–O$_c$, respectively, are consistent with previous reports [14–23]. In the $[Co(bipy)_3]^{2+}$ cation, the Co atom is six-coordinated in an octahedral coordination geometry achieved by the six nitrogen atoms of the three bipy molecules with Co–N bond lengths in the range
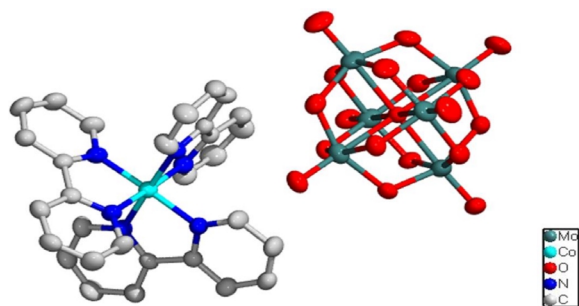
Fig. 1 (color online). ORTEP drawing of the cation and the anion in **1** with displacement ellipsoids at the 50 % probability level. Hydrogen atoms and the interstitial water molecule are omitted for clarity.
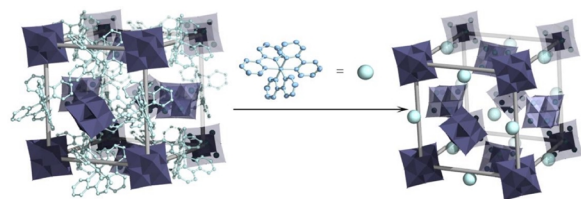

Fig. 2 (color online). View of the crystal structure of **1** (left; water molecules omitted for clarity) and schematic illustration of the NaCl topology of **1** (right).

Fig. 3 (color online). IR spectrum of compound **1**.

of 1.922(4)–1.946(4) Å. These bond lengths are comparable with those reported for other compounds containing the $[Co(bipy)_3]^{2+}$ cation [24].

The remarkable structural feature of **1** is that each $[Co(bipy)_3]^{2+}$ cation is connected to six $[Mo_6O_{19}]^{2-}$ anions while each $[Mo_6O_{19}]^{2-}$ anion is linked to six $[Co(bipy)_3]^{2+}$ cations *via* very weak hydrogen bonds (C(8)–H(8)···O(1) = 3.275(7), C(1)–H(1)···O(1) = 3.060(7) and C(8)–H(8)···O(4) = 3.372(6) Å; distances between heavy atoms) in a cubic face-centered close packing mode forming a 3D architecture with a NaCl topology, as is shown in Fig. 2. The anions are probably further connected by hydrogen bonds between the interstitial water molecule and terminal oxygen atoms of $[Mo_6O_{19}]^{2-}$, but the respective hydrogen atoms could not be located with sufficient precision.

IR spectrum

The IR spectrum of compound **1** (Fig. 3) exhibits three strong bands at 925, 780 and 605 cm^{-1}, attributed to $\nu(Mo=O_t)$, $\nu(Mo–O_b–Mo)$ and $\nu(Mo–O_c–Mo)$ vibrations in the $[Mo_6O_{19}]^{2-}$ anions, respectively. The bands at 1610, 1515, 1450, and 1300 cm^{-1} are associated with the bipy ligands [25]. The broad bands
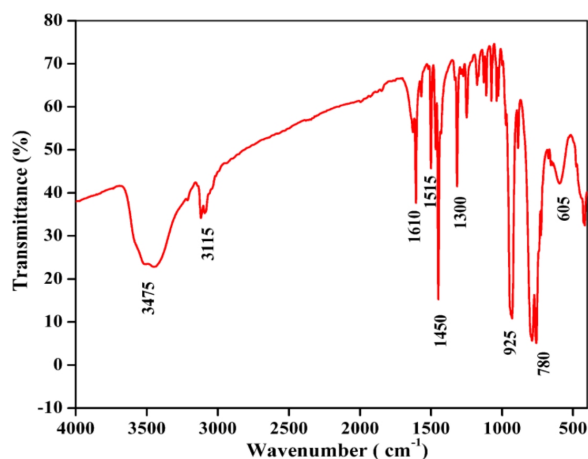
at 3475 and 3115 cm^{-1} are associated with the water molecules.

Thermal analysis

The TG analysis of **1** (Fig. 4) was performed in the temperature range of 35 to 800 °C. The first weight loss of 10.0 % (calcd. 9.86 %) in the temperature range of 35 to 365 °C corresponds to the loss of water molecules. The second weight loss of 32.6 % (calcd. 32.9 %) in the temperature range of 365 to 681 °C corresponds to the decomposition of the bipy ligands. The whole weight loss of 42.9 % is in agreement with the value of 42.7 %, calculated for the loss of all water and the decomposition of the organic moieties.
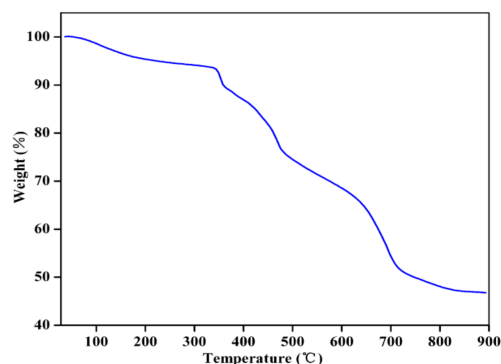

Fig. 4 (color online). TG curve of compound **1**.

Fluorescent properties of 1

The excitation and emission spectrum of **1** (Fig. 5) measured at room temperature in an aqueous solu-
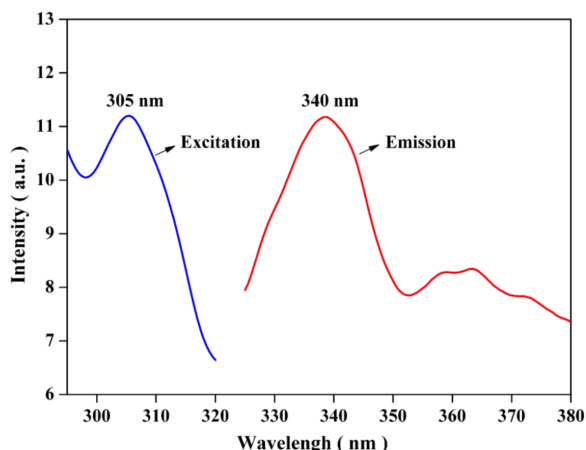
Fig. 5 (color online). Excitation and emission spectra of **1** at room temperature in aqueous solution.

tion exhibits purple photoluminescence with an emission maximum at *ca.* 340 nm, upon excitation at *ca.* 305 nm. According to the previous reports [26], the emission can be assigned to ligand-to-metal charge transfer (LMCT). This observation indicates that **1** may be a candidate for photoluminescent materials.

Electrochemical properties

The cyclic voltammetric behavior for **1**-CPE (carbon paste electrode) was studied in 1 M H_2SO_4 solution (Fig. 6). In the potential range of -0.6 to 1.0 V, there exist three redox peaks with half-wave potentials $E_{1/2}$ at -0.30 (I–I′), $+0.07$ (II–II′) and $+0.45$ V

(III–III′), which can be ascribed to redox processes of molybdenum in **1**. In addition, there is one irreversible anodic peak (IV) at $+0.76$ V, for the one electron redox process of Co^{3+}/Co^{2+} [27]. As shown in the insert of Fig. 6, when the scan rates are varied from 0.05 to 0.4 V·s^{-1}, the peak potentials change gradually: the cathodic peak potentials shift toward the negative direction and the corresponding anodic peak potentials to the positive direction with increasing scan rates. The peak currents are proportional to the scan rate, which indicates that the redox processes are surface-controlled, and the exchange rate of electrons is fast.

Electrocatalytic activity

POMs have been exploited extensively in electrocatalytic reactions and in further applications such as biosensors and fuel cells [28, 29]. Here, the reductions of hydrogen peroxide (H_2O_2) and iodate (IO_3^-) were chosen as test reactions to study the electrocatalytic activity of **1**.

As shown in Figs. 7 and 8, **1**-CPE displays good electrocatalytic activity toward the reduction of H_2O_2 and IO_3^- in 1 M H_2SO_4 solution. With addition of H_2O_2 and IO_3^-, the cathodic peak currents for I, II and III, especially peak I for H_2O_2 and peak III for IO_3^-, increase, while the corresponding anodic peak currents decrease markedly. The nearly equal current steps for each addition of hydrogen peroxide and IO_3^- demonstrate stable and efficient electrocatalytic activ-
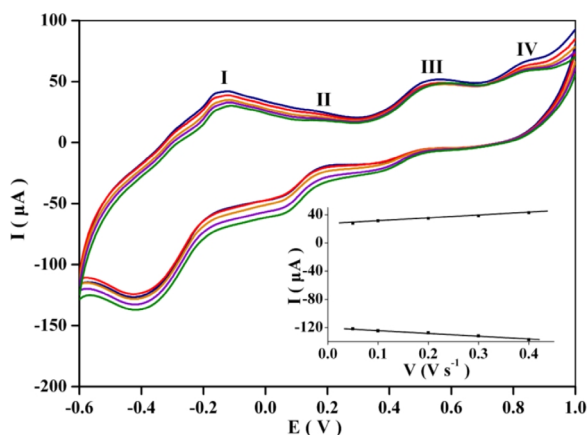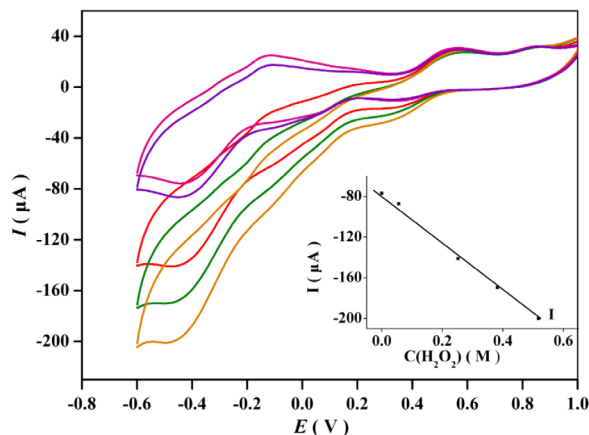

Fig. 6 (color online). Cyclic voltammograms for **1**-CPE in 1 M H_2SO_4 solution at different scan rates (from inner to outer): 0.05, 0.1, 0.2, 0.3, 0.4 V s^{-1}. The inset shows plots of the anodic and the cathodic peak currents for I against scan rates.

Fig. 7 (color online). Reduction of hydrogen peroxide at **1**-CPE in 1 M H_2SO_4 solution containing H_2O_2 in various concentrations (from top to bottom): 0, 0.06, 0.24, 0.38, 0.52 M; scan rate: 0.05 V s^{-1}. The inset shows a linear dependence of the cathodic catalytic current of wave I (I_c) with H_2O_2 concentration.

Substrate	**1**-CPE	Ref.	SiMo$_{12}$ electrode	Ref.	P$_2$Mo$_{18}$ electrode	Ref.	Table 4. Catalytic efficiencies (in %) of the
H$_2$O$_2$	244 (10 mM)	this work	14 (4 mM)	[31]	25 (5 mM)	[32]
IO$_3^-$	625 (1 mM)	this work	433 (0.3 mM)	[33]	455 (2 mM)	[34]

Table 4. Catalytic efficiencies (in %) of the modified electrode used in this study and comparison to related modified electrodes.
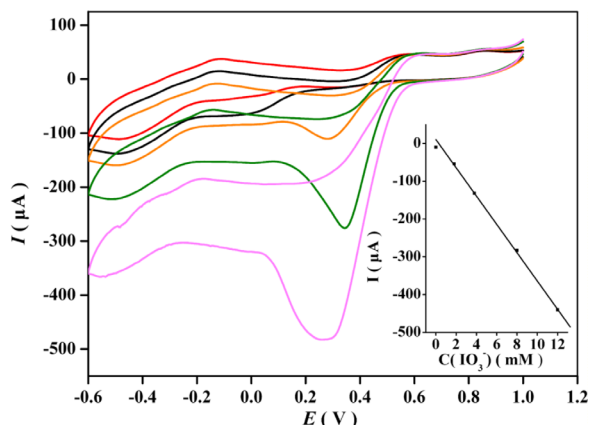

Fig. 8 (color online). Reduction of hydrogen peroxide at **1**-CPE in 1 M H$_2$SO$_4$ solution containing IO$_3^-$ in various concentrations (from top to bottom): 0, 1.8, 3.8, 8.0, 12 mM; scan rate: 0.05 V s^{-1}. The inset shows a linear dependence of the cathodic catalytic current of wave III (I_c) with IO$_3^-$ concentration.

ity of **1** immobilized in the CPE (see the inserts of Figs. 7 and 8).

Normally, the electrocatalytic activity of POMs towards oxidation or reduction of substrates can be evaluated by calculating the catalytic efficiency using Eq. 1 [30].

$$\text{CAT} = 100\% \times \frac{[I\text{p}(\text{POM, substrate}) - I\text{p}(\text{POM})]}{I\text{p}(\text{POM})} \quad (1)$$

where Ip(POM) and Ip(POM, substrate) are the catalytic currents of the POM in the absence and presence of the substrate, respectively. To make a comparison between the **1**-CPE in our work and some related molybdenum-based POM hybrids described in previous papers, the catalytic efficiencies of Mo-based modified electrodes for the reduction of hydrogen peroxide and iodate were calculated and listed in Table 4. Ip values were obtained from peak I of Fig. 7 and peak III of Fig. 8 at scan rates of 0.05 V s^{-1}. As can be seen in Table 4, the catalytic efficiency for **1**-CPE is much higher than that of reported Mo-based modified electrodes for the reduction of hydrogen peroxide and iodate. These results suggest that **1** has potential applications in the detection of hydrogen peroxide and iodate.

Conclusions

In summary, a new Lindqvist polyanion-based hybrid compound with a 3D architecture having NaCl topology has been synthesized under hydrothermal conditions. Since the hydrothermal synthesis appears to be a powerful method for obtaining new compounds of this type, we will focus on expanding this method to construct other compounds.

[1] M. T. Pope, *Heteropoly and Isopoly Oxometalates*, Springer, New York, **1983**.

[2] a) M. T. Pope, A. Müller (Eds.), *Polyoxometalate Chemistry from Topology via Self-Assembly to Applications*, Kluwer, Dordrecht, **2001**; b) E. Coronado, C. J. Gómez.García, *Chem. Rev.* **1998**, *98*, 273; c) T. Yamase, M. T. Pope (Eds.), *Polyoxometalate Chemistry for Nano-Composite Design*, Kluwer, Dordrecht, **2002**; d) A. Müller, P. Kögerler, *Coord. Chem. Rev.* **2000**, *199*, 335; e) A. Dolbecq, E. Dumas, C. R. Mayer, P. Mialane, *Chem. Rev.* **2010**, *110*, 6009.

[3] a) D. L. Long, E. Burkholder, L. Cronin, *Chem. Soc. Rev.* **2007**, *36*, 105; b) D. L. Long, R. Tsunashima, L. Cronin, *Angew. Chem.* **2010**, *122*, 1780; *Angew. Chem. Int. Ed.* **2010**, *49*, 1736.

[4] a) R. D. Gall, C. L. Hill, J. E. Walker, *Chem. Mater.* **1996**, *8*, 2523; b) Q. S. Yin, J. M. Tan, C. Besson, Y. V. Geletii, D. G. Musaev, A. E. Kuznetsov, Z. Luo, K. I. Hardcastle, C. L. Hill, *Science* **2010**, *328*, 342.

[5] Y. H. Guo, C. W. Hu, *J. Mol. Catal. A* **2007**, *262*, 136.

[6] K. Kamata, Y. Nakagawa, K. Yamaguchi, N. Mizuno, *J. Am. Chem. Soc.* **2008**, *130*, 15304.

[7] C. L. Hill, *Chem. Rev.* **1998**, *98*, 1.

[8] E. D. Clercq, *Rev. Med. Virol.* **2000**, *10*, 255.

[9] a) J. Zhang, Y. F. Song, L. Cronin, T. B. Liu, *J. Am. Chem. Soc.* **2008**, *130*, 14408; b) J. Zhang, J. Hao, Y. G. Wei, F. P. Xiao, P. C. Yin, L. S. Wang, *J. Am. Chem. Soc.* **2010**, *132*, 14; c) L. S. Long, *CrystEng-Comm* **2010**, *12*, 1354.

[10] a) A. Proust, R. Thouvenot, P. Gouzerh, *Chem. Commun.* **2008**, 1837; b) P. Mialane, A. Dolbecq, F. Sécheresse, *Chem. Commun.* **2006**, 3477; c) B. S. Bassil, S. S. Mal, M. H. Dickman, U. Kortz, H. Oelrich, L. Walder, *J. Am. Chem. Soc.* **2008**, *130*, 6696; d) J. W. Zhao, H. P. Jia, J. Zhang, S. T. Zheng, G. Y. Yang, *Chem. Eur. J.* **2007**, *13*, 10030.

[11] A. Dolbecq, E. Dumas, C. R. Mayer, P. Mialane, *Chem. Rev.* **2010** *110* 6009.

[12] R. M. Yu, X. F. Kuang, X. Y. Wu, C. Z. Lu, J. P. Donahue, *Coord. Chem. Rev.* **2009**, *253* 2872.

[13] a) D. Hagrman, C. Zubieta, D. J. Rose, J. Zubieta, R. C. Haushalter, *Angew. Chem.* **1997**, *109*, 904; *Angew. Chem., Int. Ed. Engl.* **1997**, *36*, 873; b) D. L. Long, P. Kögerler, L. J. Farrugia, L. Cronin, *Dalton Trans.* **2005**, 1372; c) D. L. Long, P. Kögerler, L. J. Farrugia, L. Cronin, *Angew. Chem.* **2003**, *115*, 4312; *Angew. Chem. Int. Ed.* **2003**, *42*, 4180; d) A. Müller, E. Beckmann, H. Bögge, M. Schmidtmann, A. Dress, *Angew. Chem.* **2002**, *114*, 1210; *Angew. Chem. Int. Ed.* **2002**, *41*, 1162; e) E. B. Wang, C. W. Hu, L. Xu, *Introduction of Polyoxometalate Chemistry*, Chemical Industry Press, Beijing, **1998**.

[14] R. N. Devi, J. Zubieta, *Inorg. Chim. Acta* **2002**, *332*, 72.

[15] V. Shivaiah, S. K. Das. *Inorg. Chem.* **2005**, *44*, 7313.

[16] Y. Xu, J. J. Lu, *Inorg. Chim. Acta* **1999**, *295*, 222.

[17] V. Shivaiah, *Inorg. Chem. Commun.* **2006**, *9*, 1191.

[18] E. Burkholder, J. Zubieta, *Inorg. Chim. Acta* **2004**, *357*, 279.

[19] J. Q. Sha, J. Peng, L. Huang, H. J. Pang, A. X. Tian, P. P. Zhang, Y. Chen, M. Zhu, *Solid State Sci.* **2009**, *11*, 417.

[20] H. Kwen, V. G. Young, Jr., E. A. Maatta, *Angew. Chem.* **1999**, *111*, 1215; *Angew. Chem. Int. Ed.* **1999**, *38*, 1145.

[21] D. Hagrman, P. J. Hagrman, J. Zubieta, *Angew. Chem.* **1999**, *111*, 3359; *Angew. Chem. Int. Ed.* **1999**, *38*, 3165.

[22] N. Avarvari, M. Fourmigue, *Chem. Commun.* **2004** 2794.

[23] M. C. Leon, E. Coronado, C. G. Saiz, C. J. G. Garcia, *J. Mater. Chem.* **2001**, *11*, 2176.

[24] J. Y. Niu, Z. J. Wang, J. P. Wang, *Pyhedron* **2004**, *23*, 773.

[25] R. G. Cao, S. X. Liu, Y. Liu, Q. Tang, L. Wang, L. H. Xie, Z. M. Su, *Solid State Chem.* **2009**, *182*, 49.

[26] M. Z. Yang, X. Y. Chen, Y. F. Liu, C. G. Zheng, *Chin. J. Spectr. Lab.* **2008**, *2*, 25.

[27] J. Q. Sha, J. Peng, J. Chen, H. S. Liu, A. X. Tian, P. P. Zhang, *Solid State Sciences* **2007**, *9*, 1012.

[28] B. Keita, P. De Oliveira, L. Nadjo, U. Kortz, *Chem. Eur. J.* **2007**, *13*, 5480.

[29] C. Pichon, P. Mialane, A. Dolbecq, J. Marrot, E. Rivière, B. Keita, L. Nadjo, F. Sécheresse, *Inorg. Chem.* **2007**, *46*, 5292.

[30] B. Keita, A. Belhouari, L. Nadjo, R. Contant, *J. Electroanal. Chem.* **1995**, *381*, 243.

[31] Z. G. Han, Y. L. Zhao, J. Peng, Q. Liu, E. B. Wang, *Electrochim. Acta* **2005**, *51*, 218.

[32] X. L. Wang, Z. H. Kang, E. B. Wang, C. W. Hu, *J. Electroanal. Chem.* **2002**, *523*, 142.

[33] H. Y. Ma, T. Dong, G. Wang, W. Zhang, F. P. Wang, X. D. Wang, *Electroanal.* **2006**, *18*, 2475.

[34] J. Y. Qu, X. Q. Zou, B. F. Liu, S. J. Dong, *Anal. Chim. Acta* **2007**, *599*, 51.